INTERNATIONAL JOURNAL OF ADVANCE RESEARCH, IDEAS AND INNOVATIONS IN TECHNOLOGY

ISSN: 2454-132X
Impact factor: 4.295
(Volume3, Issue5)
Available online at www.ijariit.com

CFD Based Investigation on Delay of Boundary Layer Separation by Active Flow Control for NACA0084M Aerofoil

Akshay Ashok Kumar
Dept of Mechanical Engineering,
kumar.akshay11293@gmail.com

Abstract: ***The unsteadiness such as boundary layer transition and turbulence at high angles of attack result in lift loss and increase in drag over an aerofoil. Numerous techniques such as suction at slots, flaps, bumps, high lift devices etc. have been developed by the scientists to control the separation delay and thereby prevent the aerodynamic losses at higher angles of attack. This research work aims at studying the effects of delaying the boundary layer separation by adopting blowing active flow control with local jets with varying velocity ratios and at different angles of attack on a 2D NACA 0084M aerofoil. Four different ratios of jet velocity (viz., 1, 2, 6 and 12) have been considered and the aerodynamic performance of each has been evaluated. The research aims to focus on the improvements in lift and drag characteristics of the above-mentioned aerofoil and identify the best possible jet velocity.***

Keywords: ***CFD, Aerodynamics, Active Flow Control, Drag, and Lift Boundary Layer Separation.***

I. INTRODUCTION

The bird has been man's inspiration to build a machine which can fly. Engineers soon realized that the cross-section of a bird's wings and the body was identified and were enthralled by the fact that it was this profile (aerofoil) which made the bird fly great heights. The National Advisory Committee for Aeronautics (NACA) soon carried out experimental analysis of various aerofoils which revolutionized aerospace industry. The aerospace industry has diversified and modern defense and commercial flights are being designed to reach greater performance levels as compared to their 20th-century counterparts. The altitude of operation has dramatically increased and long-distance air travel has become a reality.

Lift and drag are two aerodynamic loads which influence the performance of any aerospace machine. Engineers around the world have been relentlessly trying to get the maximum lift with minimum drag and have designed numerous devices which take machines closer to this ideal situation. Active flow control is one such technology which aims to delay the separation of the boundary layer from the suction face of the aerofoil at higher angles of attack thereby increasing the lift performance of the aircraft.

This research work aims at studying the effects of delaying the boundary layer separation by adopting blowing active flow control with local jets, with varying velocity ratios and at different angles of attack on the NACA0084M aerofoil. An attempt has been made to focus on the improvements in the lift and drag characteristics of the aerofoil and identify the best possible jet velocity.

II. METHODOLOGY

A. Flow Domain and Geometry

The aerofoil used for the simulation in this research work is a cambered NACA0084M and its orientation within the flow domain has been shown in figure1. The chord length is 0.381m and this scaling factor has been adopted to facilitate the validation with the experimental results of Knight.M et al [1]. The slots for the jet blowing are fixed at 53.9% of the chord length (as recommended by Knight et al [1]) and this position remains unchanged throughout the work.

The dimensions of the flow domain should be a trade-off between the complete development of the flow field and optimization of the number of elements in the grid structure. A rectangular wind tunnel which is 50m long and 20m wide has been used and the leading edge of the aerofoil was placed 10m away from the left wall and 10m below the top wall of the flow domain.

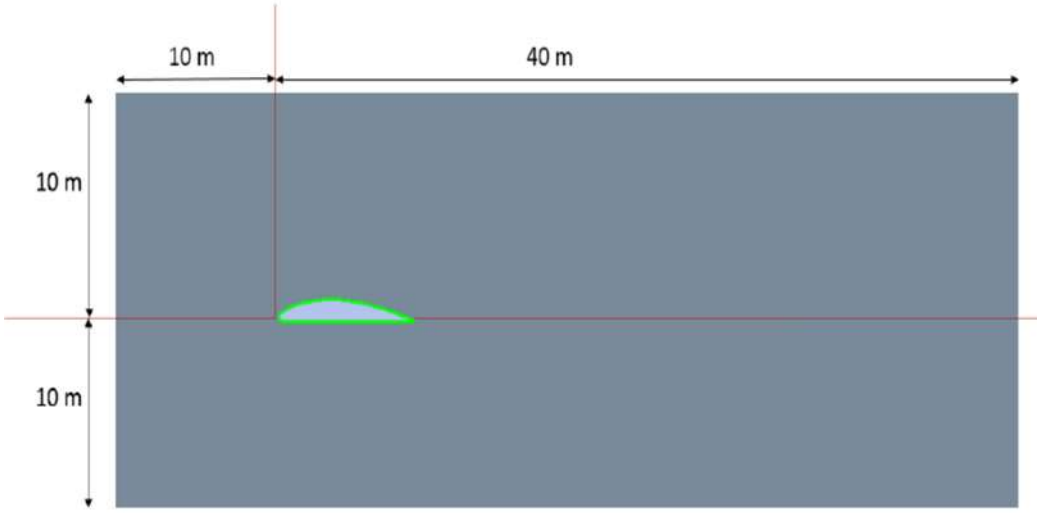

Fig. 1 Dimensions of the flow domain and the position of the aerofoil

B. Mesh Generation

The mesh used in this analysis is an unsymmetrical mesh with a high degree of refinement around the upper and lower faces of the aerofoil. Due to the limited availability of computational resources, the refinement at the air volume away from the aerofoil was given lesser importance and was left course. Pinch control was applied as a global mesh refinement and the pinch tolerance was set to 1e-6m. The mesh method is all triangles since this offered the best refinement around the aerofoil. Inflation layers have been provided with a first layer height of 2e-5m (for 35 layers at a growth rate of 1.2). It was observed that by reducing the first layer height the number of inflation layers that could be generated around the aerofoil increased. Finest possible mesh has been created around the curvatures of the aerofoil and near the trailing edge where the flow separation is likely to take place.

Since the analysis is initially performed without the active flow control, the slot on the upper surface of the aerofoil (for local jet blowing) is also treated as a wall. Thus the upper surface of the aerofoil is comprised of three edges in this case. In the second part of the report, where the active flow control is considered this slot is treated as an inlet. Thus in this situation, the upper surface has only two edges. A snapshot of the mesh is shown in figure 2.

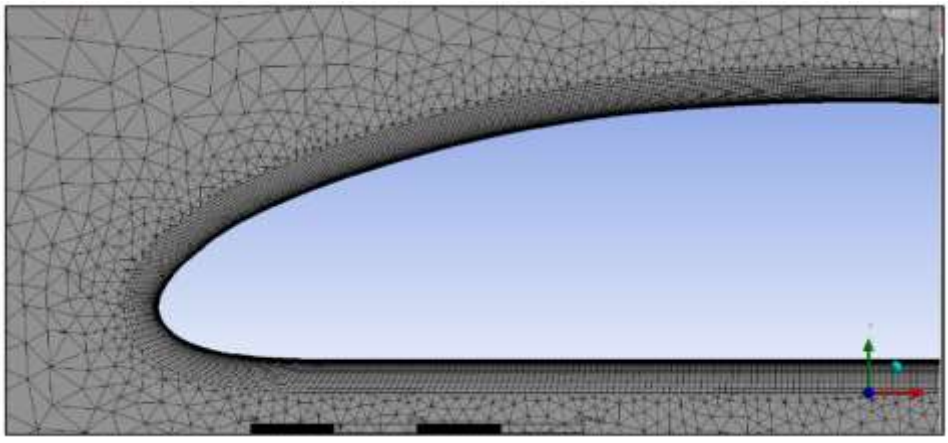

Fig. 2 Snapshot of the mesh around the aerofoil showing the inflation

C. Boundary Conditions

The Reynolds number of the free stream flow is maintained at 445000 and the characteristic length in the Reynolds number equation is assumed to be the chord length (0.381m). This leads to the estimation of the free stream velocity to be 17.06 m/s. The velocity specification method at the inlet is set to magnitude and direction, to facilitate the change in free stream velocity angle (angle of attack). The x component of the velocity is the velocity is the cosine of the angle of attack and the y component of the velocity is the sine of the angle of attack. The turbulence specification method is

turbulence intensity and length scale method since this is the best suited for external flow aerodynamics where characteristic length plays a crucial role. An extremely low value of 0.01% is set for the turbulent intensity to imitate free stream conditions. The turbulent length scale has been found to be 0.02667m (7% chord length). The following table 1 shows the boundary conditions when no active flow control is used.

TABLE I
BOUNDARY CONDITIONS FOR THE FREE STREAM

Settings	Option / Value	Justification
Velocity Specification Method	Magnitude and Direction	To facilitate the description of x and y components of velocity when the angle of attack is considered
Velocity Magnitude	17.06 m/s	Velocity corresponding to Re 445000 and chord length of 0.381m.
X component in flow direction	Cos β	Cos component of the angle of attack (β)
Y component in flow direction	Sin β	Sine component of the angle of attack (β)
Turbulence Specification Method	Intensity and Length Scale	Best suited option when systems with characteristic lengths are considered.
Turbulent Intensity	0.01%	Low turbulent intensity to imitate free stream condition
Turbulent Length Scale	0.02667m	7% of 0.381m

D. sBlowing Mechanism

Figure 3 is a pictorial representation of the blowing mechanism. V_{jet} is the velocity of the air being blown from the local jet. In this report the velocity of the local jet is fixed as one, two, six and twelve times of the free stream velocity and its effect at various angles of attack have been studied. θ_{jet} is the angle between the jet and the aerofoil surface [2]. The x and y component of the V_{jet} are represented as follows [2*]*

$$u = VR \cos(\theta_{jet} + \beta) \quad v = VR \sin(\theta_{jet} + \beta) \quad \text{(Equation 1)}$$

Where β is the angle between the jet and the free stream velocity and R is the ratio of ratio of jet velocity to the free stream velocity.

The θ_{jet} is the tan of the angle inscribed by the slot. The coordinates of the point where the slot starts are (0.205359, 0.051054) and ends are (0.20790027, 0.0508635).

$$\theta_{jet} = \tan^{-1}(dy/dx) = (0.0508635 - 0.051054) / (0.20790027 - 0.205359) = -4.28 \text{ degrees}$$

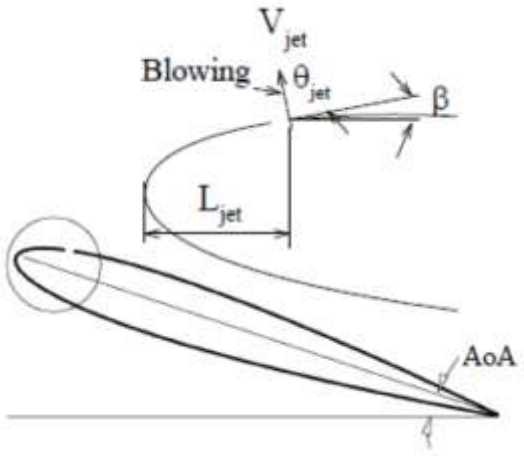

Fig. 3 Blowing Mechanism [2]

TABLE II
BOUNDARY CONDITIONS OF THE BLOWING JET AND SOLVER SETTINGS

Settings	Option / Value	Justification
Velocity Specification Method	Magnitude and Direction	To facilitate the description of x and y components of velocity when the angle of attack is considered
Velocity Magnitude	VR	V is the free stream velocity (17.06 m/s) and R is the Jet Ratio which can be 1,2,6,12
X component in flow direction	$\cos(\theta_{jet} + \beta)$	θ_{jet} = -4.28 degrees β = Angle of Attack
Y component in flow direction	$\sin(\theta_{jet} + \beta)$	θ_{jet} = -4.28 degrees β = Angle of Attack
Turbulence Specification Method	Intensity and Length Scale	Best suited option when systems with characteristic lengths are considered.
Turbulent Intensity	0.01%	Low turbulent intensity to imitate free stream condition
Turbulent Length Scale	0.02667m	7% of 0.381m
Viscous Model	SST K-w	Offers best results for external flow aerodynamics with adverse pressure gradients
PV Coupling	SIMPLE	Incompressible Flow
Spatial discretization method	Green-Gauss Node Based	Unstructured grids are used
Solution method	Second Order Upwind	More accurate than 1st order
Residual tolerance	1e-10	Need for higher degree of accuracy
Number of iterations	4500	Convergence is expected to be achieved within this

III.RESULTS

TABLE III

DRAG AND LIFT VALUES OF NACA0084M WITH AND WITHOUT FLOW CONTROL

Angle of Attack (Degrees)	No Active Flow Control		Flow Control with Velocity Ratio 1		Flow Control with Velocity Ratio 2		Flow Control with Velocity Ratio 6		Flow Control with Velocity Ratio 12	
	Cd	Cl	Cd	Cl	Cd	Cl	Cd	Cl	Cd	Cl
-6	0.0176	0.0042	0.0176	0.0042	0.0175	0.0179	0.0218	0.2477	0.0376	0.433
0	0.0178	0.582	0.0181	0.5656	0.0183	0.5766	0.0291	1.0076	0.0649	1.328
6	0.0285	1.0992	0.0317	1.0213	0.0266	1.180	0.0483	1.8867	0.1202	2.4848
9	0.042	1.262	0.0461	1.1908	0.0345	1.4713	0.0632	2.2997	0.1528	3.048
12	0.0646	1.364	0.0613	1.3808	0.0481	1.7248	0.0851	2.683	0.1952	3.5951
15	0.1018	1.378	0.083	1.5472	0.0695	1.9304	0.0530	3.2606	0.2329	3.941
18	0.1505	1.343	0.1263	1.5492	0.1024	2.0585	0.1719	3.799	0.6747	3.2023
21	0.2167	1.244	0.2088	1.3276	0.179	1.86	-	-	-	-

TABLE IV

LIFT TO DRAG RATIO OF NACA0084M WITH AND WITHOUT FLOW CONTROL

Angle of attack (Degrees)	No Active Flow Control	Flow Control with Velocity Ratio 1	Flow Control with Velocity Ratio 2	Flow Control with Velocity Ratio 6	Flow Control with Velocity Ratio 12
-6	0.239	0.238	1.022	11.33	11.515
0	32.7	31.25	31.51	34.62	20.46
6	38.56	32.217	44.36	39.06	20.67
9	30.05	25.83	42.64	36.38	19.95
12	21.11	22.52	35.86	31.5	18.42
15	13.53	18.64	27.77	28.46	16.92
18	8.92	12.26	20.10	22.10	4.74
21	5.74	6.358	10.39	-	-

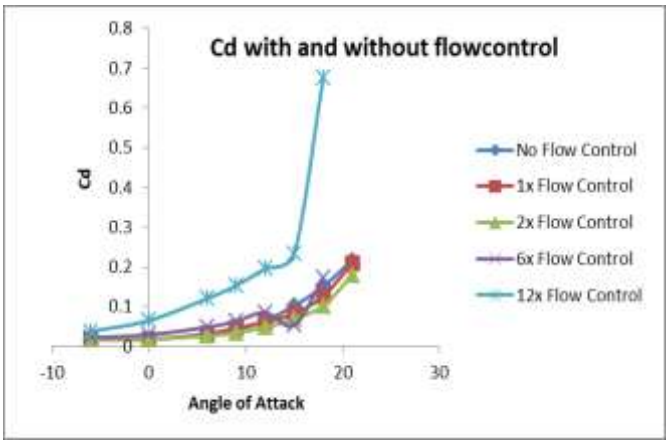

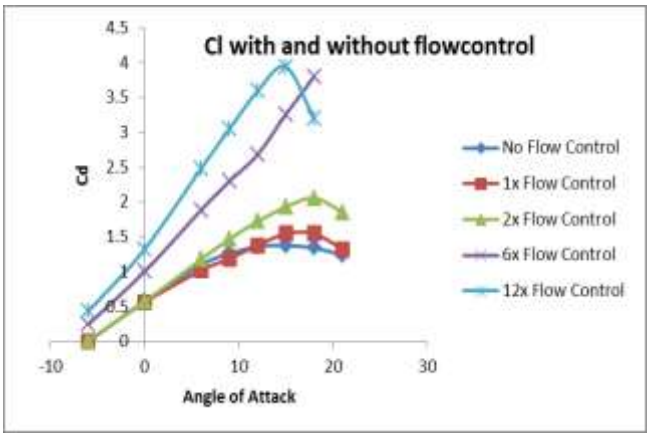

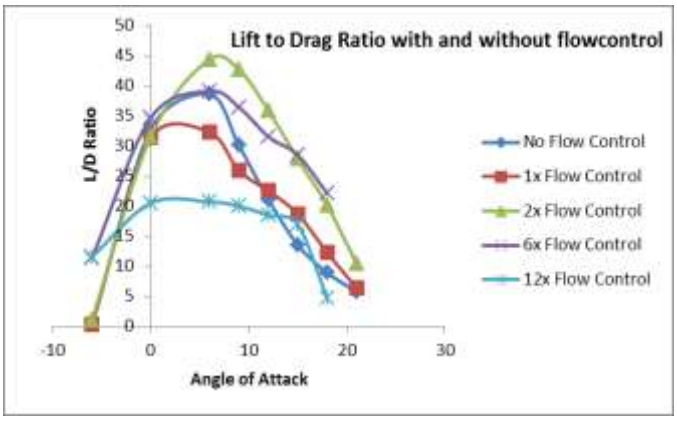

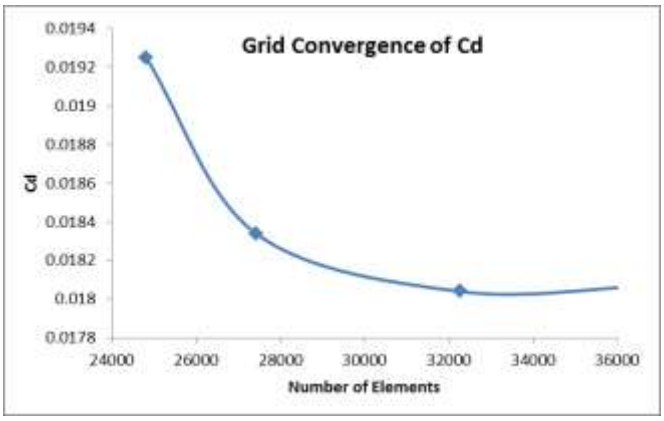

Figure 4. Cd and Cl with and without flow control Figure 5. Lift to drag with and without flow control
Figure 6. Grid convergence of Cd

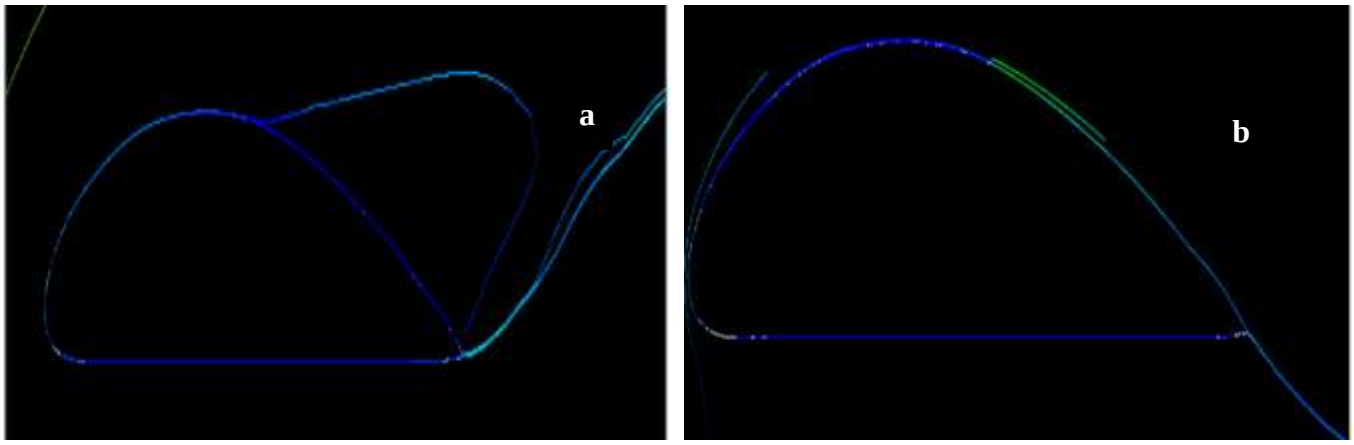

Figure 7. (a) The pathlines of velocity at AoA 15 degrees with no flow control (b) The pathlines of velocity at AoA 15 with flow control and jet ratio 12.

TABLE V
VALIDATION OF CFD SIMULATION RESULTS WITH EXPERIMENTAL RESULTS WITH NO FLOW CONTROL

Angle of Attack (Degrees)	Cd (Experimental)	Cd (CFD)	Cl (Experimental)	Cl (CFD)
-6	0.02	0.0176	0.034	0.0042
0	0.0243	0.0178	0.681	0.582
6	0.038	0.0285	1.193	1.099
9	0.0527	0.042	1.342	1.262
12	0.0606	0.0646	1.432	1.364
15	0.1202	0.1018	1.487	1.378
18	0.1583	0.1505	1.473	1.343
21	0.2713	0.2167	1.421	1.244

TABLE VI
VALIDATION OF CFD SIMULATION RESULTS WITH EXPERIMENTAL RESULTS WITH FLOW CONTROL VELOCITY RATIO 12

Angle of Attack (Degrees)	Cd (Experimental)	Cd (CFD)	Cl (Experimental)	Cl (CFD)
-6	0.1102	0.0376	0.289	0.433
0	0.1172	0.0649	1.05	1.328
6	0.1367	0.1202	1.755	2.484
9	0.1554	0.1528	2.13	3.048
12	0.1753	0.1952	2.455	3.595
15	0.2018	0.2329	2.72	3.941

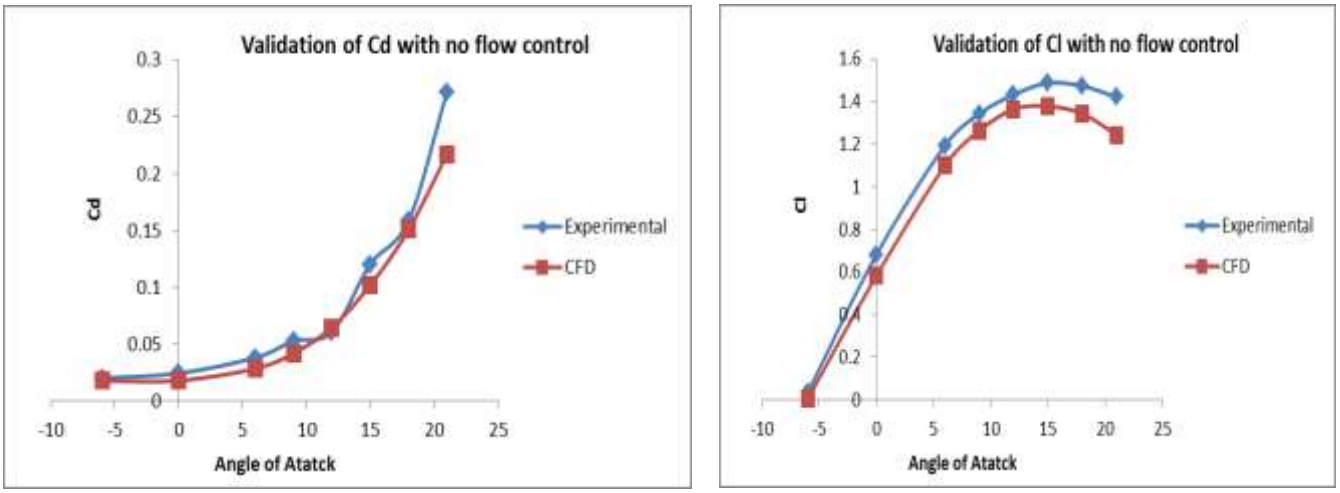

Figure 8. Validation of CFD simulation results with experimental values of Knight et al [1] with no flow control

IV. DISCUSSIONS

It has been observed from the pathlines of velocity in figure 7 that, at higher angles of attack, flow separation takes place from the upper surface of the aerofoil. From the Bernoulli's equation

$$P_\infty + \frac{\rho V_\infty^2}{2} = P + \frac{\rho V^2}{2}$$

Where P_∞ is the free stream pressure and V_∞ is the free stream velocity

$$P - P_\infty = \frac{\rho(V_\infty^2 - V^2)}{2}$$

$$\frac{P - P_\infty}{0.5\rho V_\infty^2} = \left(1 - \frac{V^2}{V_\infty^2}\right) = C_p$$

The air is a viscous medium and it induces a shear stress which is given by Newton's law of viscosity as [4]

$$\tau = \mu \left(\frac{du}{dy}\right)$$

Where µis the dynamic viscosity and the differential term is the velocity gradient

In the freestream, the flow is laminar and hence the velocity gradient is low. Consequently, the shear stress induced is fairly low and fluid layers do not experience any drag, and freely slide over one another. When the flow hits the leading edge, the flow is separated from the upper and lower surfaces of the aerofoil. At the leading edge of the aerofoil, V is equal to zero and hence Cp is equal to 1. It is highly desirable to maintain a laminar fluid flow over and above the aerofoil so that the viscous shear stress is close to zero. Such an ideal condition would have no flow separation and thereby will have zero pressure drag. But this is not possible in practical terms since the surface under consideration has a number of curves. The upper surface of the aerofoil can be divided into two parts, the part which is curved in the direction of flow (region 1 in figure 9) and the part which is curved away from the airflow (region 2 in figure 9). The region 1 causes a flow acceleration, where $V>V_\infty$ and hence $Cp<0$. In the region 2 due to surface curving away from the direction of flow, the $V<V_\infty$ and hence $Cp>0$.

Such a divergence (away from the direction of flow) in the geometry of the upper surface creates an adverse rise in the pressure gradient [4]. The pressure gradient affects the flow within the boundary layer and tends to increase the thickness of the boundary layer. Beyond a stage, due to such rapid increase in the pressure gradient, the air molecules within the boundary layer tend to reverse and move downstream [4]. Such reversal in velocity causes an enormous loss in energy and the molecules separate from the solid surface. As the angle of attack increases, this divergence in geometry is more pronounced than the one at zero degrees AoA. Thus the point of separation is attained much earlier at higher angles of attack, forming a high wake region on the upper surface (increase in pressure drag). Thus, theoretically, such reversed flow should be avoided so that the air over the upper surface of the aerofoil does not lose much of its energy and stays attached to the surface.

From the above discussion it is clear that if the air molecules moving in the region 2 of the upper surface are kept accelerated (as the molecules in the region 1 are), the molecules within the boundary layer will have sufficient energy to withstand this adverse pressure gradient and downstream motion of the fluid particles can be prevented.

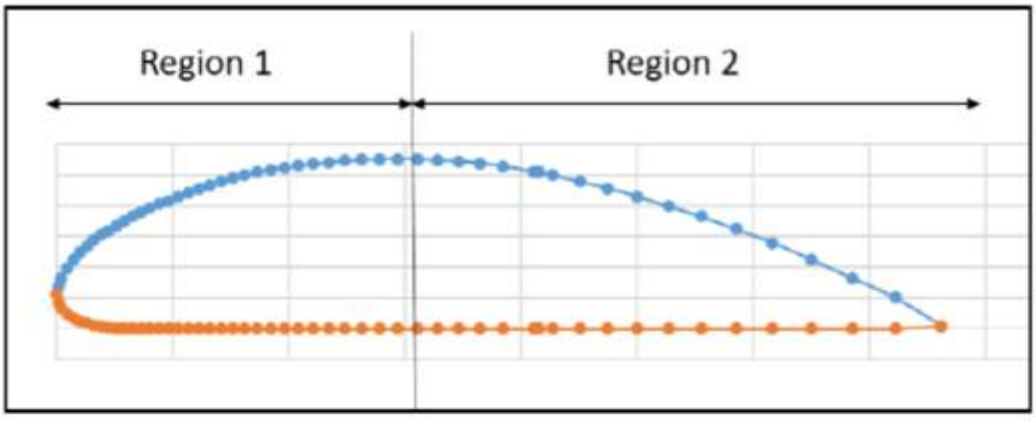

Figure 9. Two regions on the upper surface of NACA0084M

Active flow control successfully delays the boundary layer separation, by imparting some amount of energy to the decelerating molecules, thus providing them sufficient energy to stay attached to the aerofoil surface even at a high angle of attacks. This is shown in figure 7 where the pathlines of the velocity show that the flow is attached to the upper surface of the aerofoil when flow control is implemented.

B. Validation of Results

It can be seen that the values predicted by the CFD analysis are in close accordance with the experimental results of Knight et al [1]. The variation of Cl with AoA without the flow control shows that the angle of stall has been correctly determined to be 15 degrees. From figure 8 it can be observed that the experimental data suggests that with the adoption of active flow control the angle of the stall is not 15 degrees but slightly higher than that. Reliable values are not available in the experimental data at AoA 18 degrees. Similar to this result, the CFD analysis also correctly estimated that, under similar conditions, the angle of the stall is not 15 degrees which is evident from the fact that lift curve is not inflecting.

C. Comparison between Active Flow Control at different velocity ratios

The table III and IV of this report show the drag and lift values of NACA0084M with and without flow control and the following observations can be made.

- Looking at the broader perspective, the lift and drag performance at different AoA is lot favorable with flow control. This is evident from the fact that at higher jet velocity ratios, a Cl value as high as 1 is possible even at AoA 0 degrees.

- When there is no flow control, the angle of the stall for the aerofoil at Re 445000 is 15 degrees. By adopting active flow control, the angle of the stall is postponed to 18 degrees till jet ratio 6.

- It is interesting to note that the active flow control mechanism delays the boundary layer separation, which makes it possible to obtain higher lift characteristics. At lower AoA (up to 9 degrees) the lift gain is highly significant till velocity ratio 6. For example, the Cl at 6 degrees in the base condition is 1.099 and the same with active flow control with jet ratio 6 is 1.88, which is a 41% gain in lift. At the jet ratio 12, the gain is almost 55%. A parallel analysis of drag coefficient has to be made for qualitative analysis. The drag at AoA 6 degrees in base condition is 0.0285 whereas with active flow control jet ratio 6 the drag is 0.0483, which is a 41% increase in drag. But at velocity ratio 12, the drag increase is close to 77%. As a result, the advantage of lift gained at such an extremely high-velocity ratio is counterbalanced by an undesirable 77% increase in drag. **Hence at low to moderate angles of attack, the performance of a jet blowing at velocity ratio 6 is found to offer a satisfactory lift to drag characteristics.**

- It is important to make the observations at AoA 15 degrees since this is the angle of a stall in the baseline condition. Jet ratios 1 and 2 offer 11% and 28% increase in lift respectively. However, the velocity ratios 6 and 12 offer a whopping 58% and 65% increase in lift respectively. A parallel analysis of drag characteristic shows that at AoA 15 degrees Cd decreased with active flow control. The decrease in Cd at jet ratios 1 and 2 is 22% and 46% respectively as compared to the baseline condition. At jet ratio 6, the decrease in drag was almost 90%. However, at jet ratio 12, the results were not favorable and the Cd increased by 56%. Thus it can be observed that **even at high angles of attack the active flow control with jet ratio 6 offers the optimum results** (58% increase in lift and 90% decrease in drag). This result is similar to the observations made by *Goodrazi et al* [2], where it was concluded that jet ratio 6 offers the most favorable performance.

- At extremely high jet velocity ratio such as 12, the lift coefficient increases, but the drag increase is more significant than lift. As a result, the lift to drag ratio at higher angles of attack do not offer satisfactory performance.

- Though the position of the jet angle of the jet blowing mechanism has not been brought into the scope of this research, the theories discussed in the previous sections support the fact that a tangential jet is the most suited, since the shear stress due to friction acts tangentially to the aerofoil surface.

CONCLUSION

A detailed analysis of flow separation has shown that drag increase at a higher angle of attack is a problem of significance in aerofoils. It was observed that by delaying the boundary layer separation towards the trailing edge of the aerofoil, the wake region and subsequent pressure drag can be reduced at higher angles of attack. Hence, active flow control was used and air at different jet ratios was blown thus energizing the boundary layer and the point of separation was successfully delayed. As a result, the drag at a high angle of attack was reduced by up to 90% for jet ratio 6 and the angle of the stall was further delayed from 15 degrees to 18 degrees, thus improving the aerodynamic performance of the NACA0084M aerofoil.

REFERENCES

[1] Knight .M and Bamber M. J, "Wind tunnel tests on airfssoil boundary layer control using a backward-opening slot", NACA Report No.385, 1929.

[2] Goodrazi.M, Rahimi.M and Fereidouni .R, "Investigation of Active Flow Control over NACA0015 Airfoil via blowing", Internation Journal of Aerospace Sciences 1(4), pp 57-63,

[3] Douvi C. Eleni, Tsavalos I. Athanasios and Margaris P. Dionissios, "Evaluation of the turbulence models for the simulation of the flow over a National Advisory Committee for Aeronautics (NACA) 0012 airfoil", Journal of Mechanical Engineering Research Vol.4(3), pp 100-111, 2012.

[4] Wolf –Heinrich Hucho, Aerodynamics of Road Vehicles (4th edition), SAE International, ISBN 0-7680-0029-7, USA, 1998.

[5] Azim.R, Hasan .M and Mohammad Ali, "Numerical investigation on the delay of boundary layer separation by suction for NACA4412", 6th BSME International Conference on Thermal Engineering (ICTE), Procedia Engineering 105, pp 329-334, 2015.

